Brillouin study of long-wavelength spin waves in quasimonatomic Co films with uniaxial perpendicular magnetic anisotropy

Akihiro Murayama,* Kyoko Hyomi, James Eickmann, and Charles M. Falco
Optical Sciences Center and Surface Science Division of Arizona Research Laboratories, University of Arizona, Tucson, Arizona 85721
(Received 28 June 1999)

We have observed spin-wave Brillouin light scattering from ultrathin Co/Au/Cu(111) films with Co thicknesses t_{Co} down to 1 monolayer (ML) and with a 1-ML Au interlayer. The detection of a well-defined spin-wave spectrum and the field dependence of its frequency show directly long-range collective and ferromagnetic ordering in these films at room temperature. From the field dependence of the spin-wave frequency, we derive uniaxial perpendicular magnetic anisotropy constants as a function of t_{Co} with various overlayer materials, including Cu, Pd, and Au. With a Cu overlayer, we observe that the first-order perpendicular anisotropy $K_u^{(1)}$ obeys well a linear relation between $K_u^{(1)}t_{Co}$ and t_{Co} for $t_{Co} \geqq 1.5$ ML, which indicates a constant contribution of the interface anisotropy of 0.16 mJ/m^2 in addition to the volume anisotropy of 0.73 MJ/m^3. With an Au or a Pd overlayer, we find that both the interface and volume anisotropies are significantly larger than those with the Cu overlayer. We quantify magnetic inhomogeneities from the field dependence of the spectrum width. With the Au or Pd overlayer, $K_u^{(1)}$ shows a steep decrease with decreasing t_{Co} for $t_{Co} < 3.0$ ML, which agrees well with a significant increase in the structure-related magnetic inhomogeneity. We show directly that long-ranged ferromagnetic ordering exists, with the perpendicular anisotropy, in our quasimonatomic Co films thinner than 1.5 ML. $K_u^{(1)}$ for each overlayer tends to be zero at 1 ML of Co, accompanied by heavy damping of the spin wave. In addition, we find the second-order perpendicular anisotropy is still maintained with a comparable value to $K_u^{(1)}$ in such quasimonatomic Co films, indicating significant deformation of the uniaxial anisotropy.

I. INTRODUCTION

The properties of long-wavelength spin-wave excitations in monatomic or two-dimensional $3d$ ferromagnet films are one of the most important subjects in modern magnetism.[1] Monatomic Co/Cu(100) films were extensively studied and ferromagnetic ordering was reported at room temperature (RT).[2,3] Spin-wave Brillouin light scattering also was observed from such monatomic films.[4] The spin-wave Brillouin scattering technique is a very useful method for studying long-wavelength spin-wave excitations, since the wavelength of the spin wave detected by this scattering is comparable with that of the visible light used for the excitation, that is, several hundred nanometers. In addition, the sensitivity of the light scattering is sufficient for the detection of spin waves in ultrathin films less than a few monolayers (ML's). However, in contrast to the above, the Curie temperature (T_C) was reported by one group to be much lower than RT for 1.5-ML-thick Co/Cu(100).[5] Therefore, the results depend on film quality, which means that effects of the microscopic structure and its inhomogeneity on the magnetism should be taken into account for subsequent studies of monatomic films. Moreover, effects of magnetic anisotropy on long-ranged magnetic ordering are important. Theoretical work showed that long-range ordering cannot be sustained at finite temperature in a two-dimensional Heisenberg system.[6] However, later work pointed out that magnetic anisotropy would stabilize magnetic ordering as well as dipole interactions.[7–10] Experimentally, an *in situ* Brillouin study showed that ferromagnetic ordering in ultrathin Co/Cu(001) films indeed was stabilized by an in-plane anisotropy, and that where the in-plane anisotropy vanished it did so with accompanying elimination of the magnetization.[11]

More recently, Kerr hysteresis measurements showed that T_C was above or near RT in Co/Cu(111) films even with thicknesses close to 1 ML,[12] offering a good opportunity to study magnetism in quasimonatomic films at RT. In our previous study, we found Co/Au/Cu/Si(111) epitaxial films showed the narrowest width of the spin-wave Brillouin spectrum when grown with a 1-ML Au interlayer.[13] This shows directly a high degree of magnetic uniformity, which is needed for magnetic studies of quasimonatomic Co films.

From the field dependence of the spin-wave energy, we can determine magnetic properties such as magnetic anisotropies. In addition, we found that the field-dependent line broadening of the spin-wave spectrum allowed us to quantify magnetic inhomogeneities simultaneously.[14] In the present paper, we study long-wavelength spin-wave Brillouin scattering in Co/Au/Cu(111) films with Co thicknesses t_{Co} down to 1 ML and with 1 ML of an Au interlayer where the thickness was calibrated by determining the number of deposited atoms using Rutherford backscattering spectroscopy (RBS). To examine effects of an overlayer material, we deposit simultaneously Cu, Pd, or Au on graded thicknesses of Co under identical ultrahigh vacuum conditions using a movable shutter. The magnetic anisotropy constants as well as the magnetic inhomogeneities are derived as a function of t_{Co}. In this paper, we discuss magnetic properties, including the long-wavelength magnetic ordering and magnetic anisotropies in quasimonatomic Co/Au/Cu(111) films with a Cu, Pd, or Au overlayer, and their relationship to the magnetic inhomogeneities.

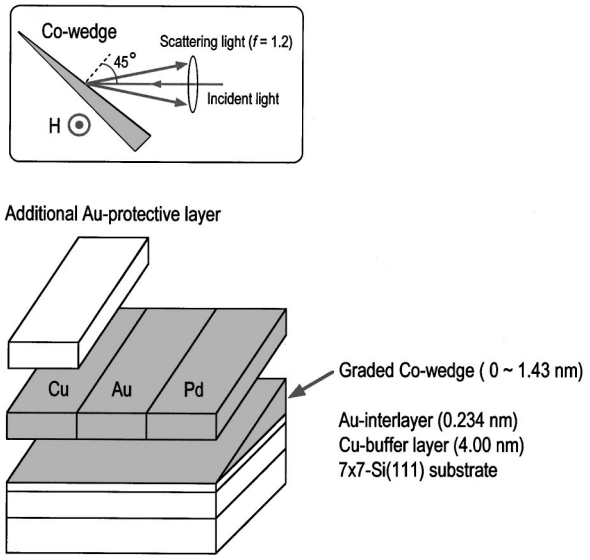

FIG. 1. Geometry of our graded Co-wedge samples. The thicknesses are in the range 0–1.43 nm corresponding to 0–7 ML, with Cu, Au, or Pd overlayers (see text). The thickness for each overlayer is 2.00 nm for Cu followed by a 3.00-nm Au protective layer, 3.00 nm for Au, and 3.50 nm for Pd. The inset shows the backscattering configuration for the spin-wave Brillouin experiment.

II. EXPERIMENT

Details of the sample preparation and Brillouin measurement are described elsewhere,[14,15] so we only describe briefly the experimental procedure which is especially important for this study. The geometry for our matrix samples is illustrated in Fig. 1. Films were deposited on a 7×7 reconstructed Si(111) surface by molecular beam epitaxy. A 4.00-nm-thick Cu buffer layer first was deposited at RT, followed by 0.23 nm of an Au interlayer. Next, a graded wedge of Co ranging from 0 to 1.43 nm was prepared using a computer-controlled movable shutter. After the formation of this Co wedge, the substrate was rotated 90°, and the three materials of the overlayer were deposited with the following procedure. First, two-thirds of the surface area of the Co wedge was covered with the shutter and a 2.00-nm-thick Cu overlayer was deposited on the uncovered portion of the Co. After forming this Cu overlayer on one-third of the sample, the shutter was moved to cover only one-third of the Co wedge and then a 3.00-nm-thick Au layer was deposited. In addition to forming the Au overlayer on the center one-third of the sample, the Au also formed a protective covering on the initial Cu overlayer. The Au protective layer for the Cu overlayer was necessary since we observed oxide formation on a bare Cu surface. Next, the substrate was rotated 180°. The part of the Co wedge with the Au and Au/Cu overlayers was covered with the shutter again and finally a 3.50-nm-thick Pd overlayer was deposited on the remaining bare Co. Electron-beam guns controlled by optical-feedback monitors were used for the depositions with rates of 0.04 nm/sec for Cu, and 0.01 nm/sec for Au, Co, and Pd, which were determined with an absolute accuracy within $\pm10\%$ using RBS. We controlled the film thickness by means of the deposition time, that is, the number of deposited atoms. The average number of monolayers was calculated using bulk values of the lattice constants. Also, we independently confirmed the Co thickness using a planar sample with $t_{\mathrm{Co}}=10$ ML by means of both a low-angle x-ray diffraction and a cross-sectional high-resolution transmission electron microscope (TEM) image. These results showed an interface roughness of 1 ML for this 10-ML film of Co. The thickness distribution also was evaluated by RBS and was within $\pm2\%$ for the wedge. We also used *in situ* reflected high-energy electron diffraction (RHEED) and Auger electron spectroscopy (AES) to evaluate the film structure and quality.

A tandem $6(3+3)$-pass Fabry-Perot interferometer was used *ex situ* to detect the spin-wave scattering at RT. A backscattering geometry was used with an incidence angle of 45°, as shown in Fig. 1. The f number of the collecting lens was 1.2 and the beam radius of incident laser light was 0.7 mm. The radius of the focused spot was estimated as a few tens of micrometers after adjusting the focal point using a microscope. A solid-state detector with a quantum efficiency of 44% and the dark count of 2.2 counts/sec was used. The incident laser power was 200 mW. Any damage of the film was not seen with this incident power, in addition to the repeatability of the spin-wave spectrum. The full width at half maximum (FWHM) of the Rayleigh peak was 0.5 GHz and the free spectral range was 37.5 GHz. All the Brillouin data were measured using a single specimen with matrix samples, as shown in Fig. 1. The thickness gradient of the Co wedge was 3 mm/ML, which was sufficiently larger than the light spot for the Brillouin excitation. This meant that thickness variations across the beam were negligible. The saturation magnetization M_s at RT was measured using 8×8-mm^2 planar samples by a highly sensitive vibrating sample magnetometer (VSM) with a sensitivity of 2×10^{-6} emu.

III. RESULTS

A. Sample quality

We observe narrow-streak RHEED patterns through deposition of each layer, which indicates an epitaxial fcc (111) structure with high crystallinity and a flat surface. Since it was difficult to distinguish the Co(0001) stacking from Co(111) using this RHEED technique, we confirmed directly the Co(0001) stacking on a 1-ML Au interlayer by means of a cross-sectional high-resolution TEM image. The formation of a 1.5-nm-thick Cu silicide with the crystal plane rotated 30° around the [111] axis from the Si substrate is observed during the initial growth of the Cu buffer layer, in agreement with previous results using TEM.[16] The average in-plane lattice constant of Au on the Cu buffer layer increases monotonically with increasing Au thickness up to 5 ML, at which point it has attained its bulk value. We also find that the Co layer is expanded by the Au interlayer.[14] Figure 2 shows the lattice constant of Co and the specular beam intensity of RHEED as a function of t_{Co}. With the combination of the incidence angle of 0.5° and the acceleration voltage of 15 kV, the skin depth of the e beam is estimated to be less than several ångstroms. As can be seen, the Co layer is expanded due to its epitaxial growth on the Au interlayer, and the lattice constant can be well expressed by a $1/t_{\mathrm{Co}}$ dependence except for initial two data points. This t_{Co} dependence can be understood as a relaxation of misfit strain,[17] and the critical thickness t_c at which point the misfit

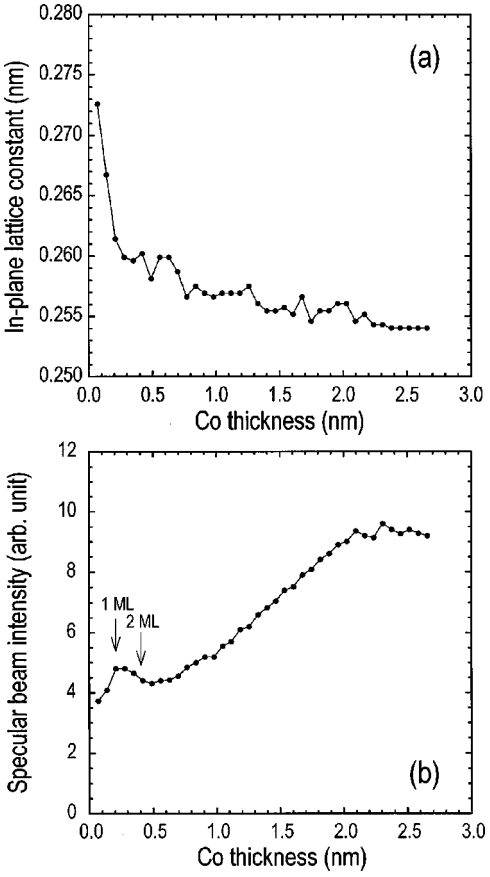

FIG. 2. (a) In-plane lattice constant of Co grown on Au/Cu(111) with 1 ML Au and (b) specular beam intensity of RHEED as a function of Co thickness. These data were obtained from intensity line scans of RHEED images, with the lattice constant calibrated by the lattice spacing of the Si(7×7) substrate surface. RHEED images were continually captured in a planar sample. The direction of the *e* beam was closely parallel to the $[1\bar{1}0]$ axis. The bulk lattice constants are $a_{\mathrm{fcc\ Au}}=0.2884$ nm and $a_{\mathrm{hcp\ Co}}=0.2507$ nm, respectively.

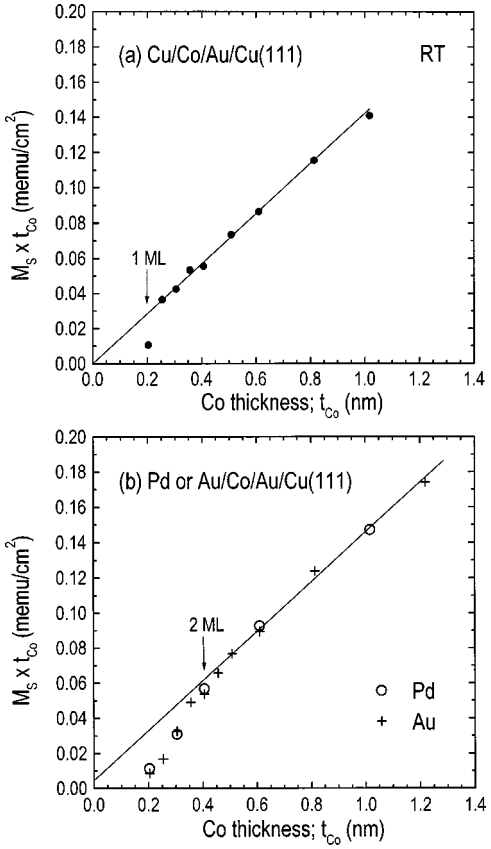

FIG. 3. Saturation magnetization M_s multiplied by the thickness of Co, t_{Co}, as a function of t_{Co}, with (a) a Cu overlayer (2.00 nm with 3.00-nm-thick Au) and (b) a Pd (3.50 nm) or an Au overlayer (3.00 nm). The solid line is a linear fit of (a) $M_s t_{\mathrm{Co}}=(1422\ \mathrm{Gauss})t_{\mathrm{Co}}$ for Cu and (b) $M_s t_{\mathrm{Co}}=(1422\ \mathrm{Gauss})t_{\mathrm{Co}}+5\times10^{-6}$ emu/cm^2 for Pd or Au, where the bulk value of Co is 1422 Gauss at RT.

strain starts to relax is nearly equal to 0 ML. On the other hand, a strong oscillation of the specular beam intensity as a function of t_{Co} is not observed, which shows that the growth mode of Co/Au/Cu(111) is not a layer-by-layer growth. The RHEED oscillation was also not to be observed for Co/Cu(111) films.[12] However, the specular beam intensity from our ultrathin Co even with a thickness of 1 ML is relatively high, equivalent to that from Co with a thickness of several ML's. After the deposition of several ML's of Co, the intensity starts to increase, saturating at 10 ML. Therefore, we conclude that the film quality of our quasimonatomic Co is not significantly degraded, in comparison with that of several ML's of Co, while the structural imperfections such as voids and island formation in part can be expected. This t_{Co} dependence of the RHEED intensity is qualitatively different from that of Co/Cu(111) reported in Ref. 12, where the specular beam intensity decreased steeply with increasing t_{Co}. This difference of the t_{Co} dependence of the RHEED intensity is possibly due to the use of the Au interlayer in our samples. In addition, AES analysis reveals no contamination in the Co layer within a sensitivity of 3%.

Figure 3 shows M_s results as a function of t_{Co} for each overlayer. With a Cu overlayer, the bulk value of M_s is obtained for $t_{\mathrm{Co}}\geqq1.3$ ML. However, for Pd or Au overlayers, a monotonic decrease in M_s with decreasing t_{Co} for $t_{\mathrm{Co}}<2.5$ ML is observed, in addition to a small contribution of magnetization of 5×10^{-6} emu/cm^2 possibly due to the magnetic polarization of the overlayer material near the upper interface between Co and the overlayer.

Figure 4 shows spin-wave Brillouin spectra from ultrathin Co films, $1\leqq t_{\mathrm{Co}}\leqq2$ ML, with a Cu overlayer. The sharp peak directly indicates a well-defined spin-wave excitation at RT with a wavelength of 376 nm, which is accessible by the laser light of the wavelength of 532 nm and an incidence angle of 45° to the film surface in this experiment. As can be seen, we find the spin-wave scattering intensity from Co with $t_{\mathrm{Co}}<1.1$ ML is significantly lower than that with $t_{\mathrm{Co}}\geqq1.1$ ML for this Cu overlayer. We note that we did not observe a spin-wave spectrum from Co with $t_{\mathrm{Co}}\leqq1.1$ ML with either Pd or Au overlayers. Therefore, this suggests that this 1.1 ML is a critical thickness for the observation of well-defined spin-wave excitations.

B. Calculation procedure

Before discussing experimental results for the field dependence of the spin-wave Brillouin frequency, we first describe our calculation procedure. We have included effects of both the dipole and exchange fields in the calculation of spin-

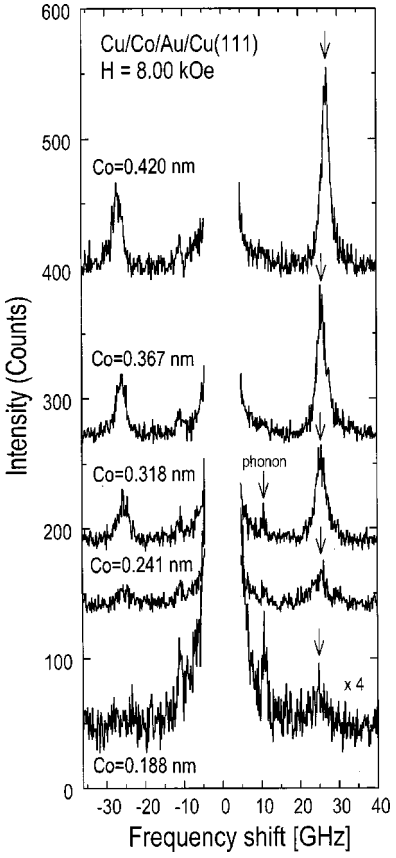

FIG. 4. Spin-wave Brillouin spectra from ultrathin Co films with various thicknesses down to ~1 ML, with a Cu overlayer with the thickness of 2.00 nm. An external field of 8 kOe was applied parallel to the film plane. The free spectral range was 37.5 GHz, and each spectrum was accumulated using 1024 channels with total dwell time of 2 sec/channel. An arrow indicates the anti-Stokes spin-wave Brillouin peak. A weak peak due to a surface acoustic phonon is also indicated, which cannot be eliminated by the cross-polarization configuration.

wave frequency, which are caused by a fluctuation of the magnetization due to the surface spin wave observed by this light scattering method. Both corrections are a function of t_{Co} and are necessary for precise discussion of the t_{Co} dependence of magnetic properties. We apply the procedure of Cochran *et al.* for the spin-wave calculation[18] to our system. A magnetic thin film with thickness d lies in the xz plane. The external field H is applied along the x axis, ϕ is the angle of the magnetization M with respect to the x axis, θ is the angle of the magnetization with respect to the z axis, ξ and η are small angles of deviation of the magnetization from its equilibrium position, and ζ is the equilibrium direction of the magnetization vector. The equations of motion for small deviation of the magnetization can be expressed as follows,

$$M\dot{\eta} = -\gamma \partial E/\partial \xi + T_\eta, \tag{1}$$

$$M\dot{\xi} = \gamma \partial E/\partial \eta + T_\xi, \tag{2}$$

where T_η and T_ξ are the torque per unit area generated by the field due to the small deviation of the magnetization and $\gamma = g|e|/2\,\mathrm{mc}$. We obtain expressions for the torque as follows,

$$T_\eta = 4\pi M^2 \cos^2\phi (1 - qd/2)\,\eta\gamma, \tag{3}$$

$$T_\xi = -2\pi M^2 qd\,\xi\gamma, \tag{4}$$

where q is the wave vector of the spin wave, which is parallel to the z axis. The free energy per unit volume of the system can be expanded for small ξ and η as follows:

$$E = E_0 + (E_{\xi\xi}\xi^2 + 2E_{\xi\eta}\xi\eta + E_{\eta\eta}\eta^2)/2. \tag{5}$$

Since ξ and η are characterized by time and space variations as $e^{i\omega t}$ and e^{iqx},

$$(\omega/\gamma)^2 = (E_{\xi\xi}E_{\eta\eta} - E_{\xi\eta}^2)/M^2 + 2\pi qd(E_{\eta\eta} - E_{\xi\xi}\cos^2\phi) + O((qd)^2). \tag{6}$$

An exchange field is included to the torque equations in the same manner. The additional term caused by the exchange contribution can be expressed using an exchange stiffness constant A as follows:

$$2Aq^2[E_{\eta\eta} + E_{\xi\xi} + 2\pi M^2 qd(1 - \cos^2\phi)]/M^2 + O((Aq)^2). \tag{7}$$

The equilibrium position of the magnetization can be derived from angular differential of the free energy and, as a result, $\theta = \pi/2$ in this system. Neglecting higher order terms, $O((qd)^2)$ and $O((Aq)^2)$, we obtain

$$(\omega/\gamma)^2 = (E_{\theta\theta}E_{\phi\phi} - E_{\theta\phi}^2)/M_s^2 + 2\pi qd(E_{\phi\phi} - E_{\theta\theta}\cos^2\phi) + 2Aq^2[E_{\theta\theta} + E_{\phi\phi} + 2\pi M_s^2 qd(1 - \cos^2\phi)]/M_s^2, \tag{8}$$

where the second and third terms correspond to the dipole and exchange contributions, respectively.

The free energy per unit volume of the system can be expressed as $E = E_{\mathrm{Zeeman}} + E_{\mathrm{magnetostatic}} + E_{\mathrm{anisotropy}}$. Within our experimental resolution of 0.2 GHz for $t_{\mathrm{Co}} \geqq 2.0$ ML and 0.5 GHz for $t_{\mathrm{Co}} < 2.0$ ML, respectively, in the Co/Au/Cu(111) plane, the spin-wave frequency is independent of the angle between the in-plane crystal axis and the applied field. Thus the in-plane crystal anisotropy is omitted from our calculation, and the uniaxial anisotropy contribution per unit volume is expressed in the free energy as $E_{\mathrm{anisotropy}} = -K_u^{(1)}\sin^2\phi - K_u^{(2)}\sin^4\phi$. A positive value of each anisotropy constant indicates perpendicular anisotropy. Therefore,

$$E = -HM_s\cos\phi + (2\pi M_s^2)\sin^2\phi - K_u^{(1)}\sin^2\phi - K_u^{(2)}\sin^4\phi. \tag{9}$$

Since the demagnetizing factor is not equal to 1 for ultrathin films thinner than several ML's, an effective magnetization field is also introduced as follows,

$$(4\pi D_\perp M_s)_{\mathrm{eff}} = 4\pi D_\perp M_s - 2K_u^{(1)}/M_s, \tag{10}$$

where $D_\perp$, the effective demagnetizing factor, is numerically calculated for a fcc (111) or hcp (0001) plane.[19–21] If this effective magnetization field is negative, M_s is oriented perpendicular to the film plane without an external field. When the applied in-plane field is equal to $(4\pi D_\perp M_s)_{\mathrm{eff}}$, the effective field acting on the precessing magnetization vanishes. For applied fields larger than $|(4\pi D_\perp M_s)_{\mathrm{eff}}|$ the

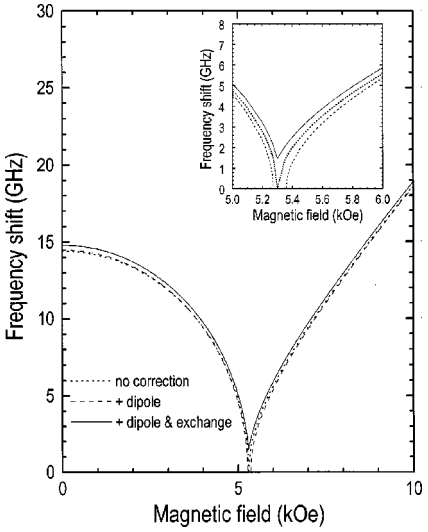

FIG. 5. An example of the spin-wave calculation as a function of external field, which is made for 0.408-nm-thick Co with a 3.00-nm-thick Au overlayer. Parameters are as follows: $M_s = 1394$ G, $g = 1.94$, $(4\pi D_\perp M_s)_{\text{eff}} = -5.30$ kOe, $A = 2.85 \times 10^{-6}$ erg/cm (Refs. 22 and 23), and $K_u^{(2)} = 0$. The dotted line shows the result without dipole and exchange contributions. The effects of dipole (dashed line), or dipole and exchange fields (solid line) are also indicated. The inset shows the detailed field dependence of the spin-wave frequency around the critical field of 5.30 kOe.

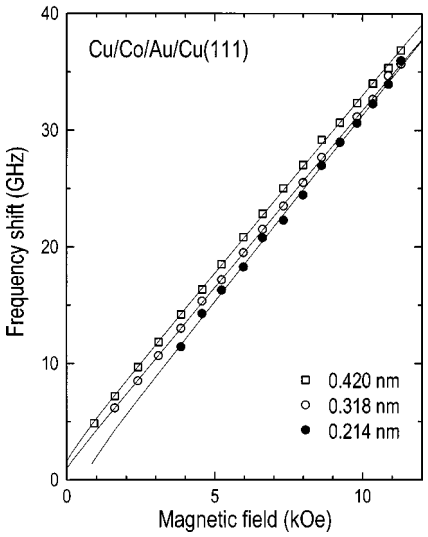

FIG. 6. Field dependence of spin-wave Brillouin frequency for various thicknesses of ultrathin Co films with 2.00-nm-thick Cu overlayers. The solid lines show the least-squares fit for the field dependence of the spin-wave frequency, where the anisotropy constants and the g factor are the fitting parameters. A monotonic increase in the spin-wave energy with increasing field indicates that the magnetization is in-plane.

magnetization is oriented parallel to the external field in the film plane. Finally, the spin-wave frequency was calculated as a function of H using Eq. (8). Figure 5 shows an example for the calculation made for 2 ML of Co with an Au overlayer. The effect of the intralayer exchange interaction on the spin-wave frequency appears, which is similar to the calculation result obtained by Stamps and Hillebrands.[23] As can be seen, the effects of both the dipole and exchange fields are not so significant for this ultrathin film. We are able to fit the measured field dependence of the spin-wave frequency in each sample using the above procedure.

C. Results and discussion

The field dependence of the spin-wave frequency for ultrathin Co films thinner than 2 ML with a Cu overlayer is shown in Fig. 6. As can be seen, the spin-wave frequency increases monotonically with increasing field, showing that the magnetization is in the film plane. This field dependence of the spin-wave energy shows a ferromagnetic behavior of the magnetization in these quasimonatomic Co films. On the other hand, with Pd or Au overlayers, an effect of the perpendicular anisotropy becomes more apparent in this ultrathin film region. The field dependence of the spin-wave frequency for a Pd overlayer is shown in Fig. 7. A minimum of the spin-wave frequency exists, indicating a critical field H_{crit} at which the magnetization starts to incline toward an out-of-plane position as the field decreases. Also, the effective field acting on the magnetization in the absence of exchange is a minimum at H_{crit}. As described above, the existence of a frequency that does not reach zero at the minimum at H_{crit} is attributed to the dipole and exchange energy contributions. When the external field is less than H_{crit}, the spin-wave frequency increases with decreasing field, which is interpreted as the magnetization inclining from the film plane under a weak external field due to the strong perpendicular anisotropy. In addition, the contribution of $K_u^{(2)}$ is also included. The angle between the magnetization and the film plane is determined by the competition between the perpendicular anisotropy and the in-plane external field. The contribution of $K_u^{(2)}$ appears in the field dependence of the spin-wave fre-

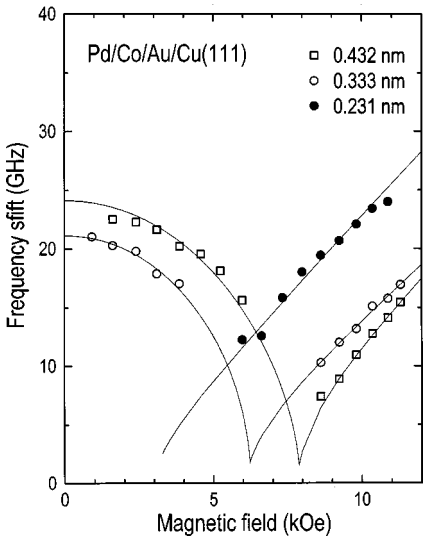

FIG. 7. Field dependence of the spin-wave Brillouin frequency in quasimonatomic Co films with a 3.50-nm-thick Pd overlayer. The solid lines are the calculated best fits. The critical field appears as a minimum of the frequency, where the transition between in-plane and out-of-plane magnetizations occurs. Below this field, the magnetization inclines from the film plane due to the perpendicular anisotropy. As discussed in the text, the nonzero behavior of the frequency at the critical field is due to both the dipole and exchange contributions, depending on the Co thickness.

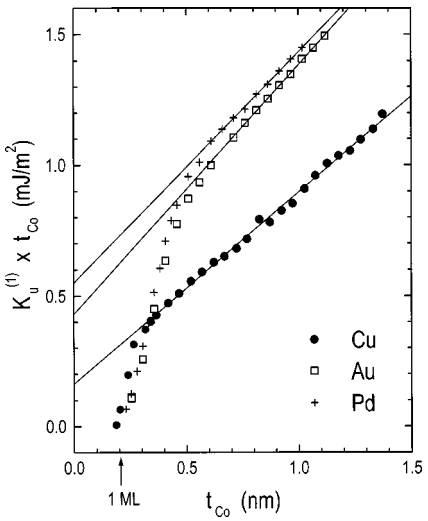

FIG. 8. Product of the perpendicular anisotropy constant $K_u^{(1)}$ determined from spin-wave measurements and t_{Co} as a function of t_{Co}, with various overlayer materials. The thickness for each overlayer is 2.00 nm for Cu with 3.00-nm-thick Au, 3.00 nm for Au, and 3.50 nm for Pd. Solid lines are least square fits for $t_{\mathrm{Co}} \geqq 1.5$ ML for the Cu overlayer and for $t_{\mathrm{Co}} \geqq 3$ ML for the Pd or Au overlayer. From the linearity $K_u^{(1)} t_{\mathrm{Co}} = K_{u,I}^{(1)} + K_{u,V}^{(1)} t_{\mathrm{Co}}$, the interface anisotropy $K_{u,I}^{(1)}$ and the volume anisotropy $K_{u,V}^{(1)}$ are determined as $K_{u,I}^{(1)} = 0.16\ \mathrm{mJ/m^2}$ and $K_{u,V}^{(1)} = 0.73\ \mathrm{MJ/m^3}$ for the Cu overlayer, $K_{u,I}^{(1)} = 0.43\ \mathrm{mJ/m^2}$ and $K_{u,V}^{(1)} = 0.95\ \mathrm{MJ/m^3}$ for the Au overlayer, and $K_{u,I}^{(1)} = 0.55\ \mathrm{mJ/m^2}$ and $K_{u,V}^{(1)} = 0.88\ \mathrm{MJ/m^3}$ for the Pd overlayer, respectively. Experimental errors are less than 0.04 mJ/m^2.

quency below H_{crit}, with $t_{\mathrm{Co}} < 2.5$ ML for a Pd or an Au overlayer, where the strong perpendicular anisotropy gives $(4\pi D_{\perp} M_s)_{\mathrm{eff}} < 0$.

From the field dependence of the spin-wave frequency, we derive magnetic parameters as a function of t_{Co} for each overlayer, including the $K_u^{(1)}$, $K_u^{(2)}$, and g factor. Figure 8 shows the result for $K_u^{(1)}$, where the product of $K_u^{(1)} t_{\mathrm{Co}}$ is plotted as a function of t_{Co}. We observe a linear relation for each overlayer, except for the ultrathin-film region. This linear relation indicates the existence of an interface anisotropy that can be phenomenologically represented as $K_u^{(1)} t_{\mathrm{Co}} = K_{u,I}^{(1)} + K_{u,V}^{(1)} t_{\mathrm{Co}}$, where the first term is the sum of the interface anisotropy and the $K_{u,V}$ term is the volume anisotropy. From this linearity we can determine the value of interface anisotropy from the intercept on the vertical axis, as well as the volume anisotropy from the gradient. The effect of misfit strain on the anisotropy has been discussed previously based on a critical layer thickness t_c between coherent and incoherent film growth in the epitaxial system as follows:[24,25]

$$K_I = K_N + K_{\lambda}, \quad K_V = K_{MC} - 2\pi M_s^2 \qquad \text{for } t_{\mathrm{Co}} > t_c \tag{11}$$

$$K_I = K_N, \quad K_V = K_{MC} + K_{ME} - 2\pi M_s^2 \qquad \text{for } t_{\mathrm{Co}} < t_c, \tag{12}$$

where K_N is the Néel-type surface anisotropy and K_{λ} is the magnetoelastic contribution in the interface anisotropy. Since t_c is nearly equal to 0 ML in our films, Eq. (11) is applicable. This agrees with our experimental result in part, where $K_V = 0.73\ \mathrm{MJ/m^3}$ found for the Cu overlayer is comparable with the value of 0.56 MJ/m^3 determined for well-characterized hcp Co.[26] This indicates that the crystallinity of Co is stable and bulklike for $t_{\mathrm{Co}} \geqq 1.5$ ML with a Cu overlayer and also the interface-induced misfit strain does not significantly affect the volume anisotropy. Additionally, the constant value of K_I means the atomic-scale quality of the interface is identical for $t_{\mathrm{Co}} \geqq 1.5$ ML.

On the other hand, capping with a Pd or an Au overlayer results in a K_V that is significantly higher than that with Cu, as well as K_I. The only possible source for this increase in the volume anisotropy is the additional strain due to the deposition of Pd or Au on Co, since the lattice constants of Pd and Au are markedly larger than that of Co (8% and 14% larger, respectively). Previous RHEED analysis showed that Au growth on Co was incoherent and stress-free for coverages greater than 1 ML.[27] If we assume the Pd or Au overlayer induces dislocation-free and thus thickness-independent strain inside Co, Eq. (12) shows it is reasonable to apply the framework of strain-modified volume anisotropy to the result. For the increase in the interface anisotropy with the Pd or Au overlayer, additional formation of dislocations near the upper interface between Co and the overlayer can be pointed out as a possible origin, in addition to the change in K_N. This dislocation formation means a thickness-dependent strain relaxation will occur, and this can contribute to K_I. In addition, as can be seen from Fig. 8, $K_u^{(1)}$ starts to degrade from linearity at 3 ML of Co with a Pd or Au overlayer. This critical thickness of Co for the degradation of anisotropy is slightly larger than that for the degradation of M_s. This degradation of $K_u^{(1)}$ was previously observed below several ML's of Co in Co/Au multilayers and the effect of misfit strain was discussed.[17,28] However, in our single films, t_c is close to 0 ML and it does not agree with the thickness at which the anisotropy starts to degrade. Also, as shown above, we find that the Co thickness at which $K_u^{(1)}$ starts to degrade depends strongly on the overlayer material.

Next we show effects of structural and resultant magnetic inhomogeneities on the magnetic anisotropy. As shown in an inset of Fig. 9, we see a field-dependent broadening of the spectrum width Δf around H_{crit}. This behavior is quantitatively explained by assuming a distribution of the effective magnetization field as follows:

$$\Delta f = \Delta f_0 + \Delta(4\pi D_{\perp} M_s)_{\mathrm{eff}} \{\partial f / \partial (4\pi D_{\perp} M_s)_{\mathrm{eff}}\}, \tag{13}$$

where f is the spin-wave frequency. The value of $(4\pi D_{\perp} M_s)_{\mathrm{eff}}$ is determined from the fitting for the spin-wave frequency. The term Δf_0 indicates the field-independent width, possibly due to structure-related inhomogeneities such as defects. The term $\Delta(4\pi D_{\perp} M_s)_{\mathrm{eff}}$ means the degree of distribution of the effective magnetization field, that is, $K_u^{(1)}$. We find that these parameters depend strongly on t_{Co} in our single-crystal films. The result for an Au overlayer is shown in Fig. 9. As can be seen, Δf_0 starts to increase rapidly below 3 ML of Co, which coincides well with the deviation of $K_u^{(1)}$ from linearity as shown in Fig. 8. We obtained a similar dependence for Pd overlayers. Therefore, we conclude that the significant degradation of $K_u^{(1)}$ is due to the degradation of the film structure resulting from capping with the Au or Pd overlayer. We note that the effect of an Au

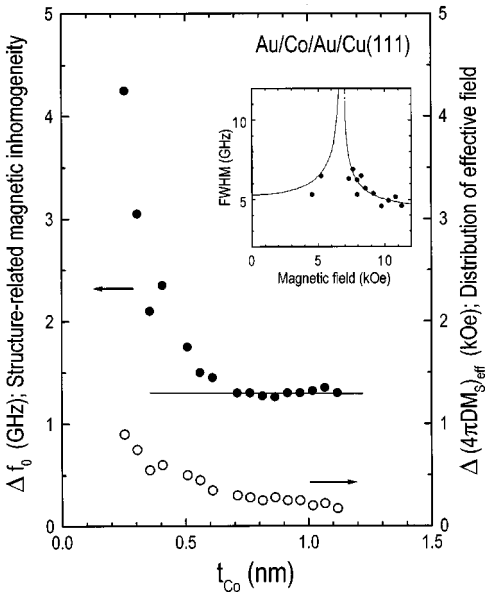

FIG. 9. Parameters indicating magnetic inhomogeneities, Δf_0 and $\Delta(4\pi D_\perp M_s)_{\rm eff}$, as a function of $t_{\rm Co}$, which are determined from the field dependence of the spectrum width (as shown in inset).

or Pd overlayer on $K_u^{(1)}$ is different between $t_{\rm Co}\geqq 3$ ML and $t_{\rm Co}<3$ ML. The former thickness range shows large constant volume and interface anisotropies, while the latter range shows a degradation of those anisotropies. Therefore, we conclude for $t_{\rm Co}\geqq 3$ ML, the epitaxial growth of the overlayer causes both a thickness-independent strain and a thickness-dependent dislocation formation near the upper interface of Co, which are responsible for the magnetoelastic volume anisotropy and the interface anisotropy, respectively. From our Brillouin result for $t_{\rm Co}\geqq 3$ ML, the structure-related inhomogeneity is relatively small and constant, which means that the effects of additional strain are uniform and thus can contribute to the enhancement of anisotropies. In contrast, for $t_{\rm Co}<3$ ML, the additional strain and dislocation formation are significantly inhomogeneous. Therefore, defects and/or an inhomogeneous distortion of the lattice structure of Co is responsible for the degradation of $K_u^{(1)}$. In Co/Au superlattices with 2-nm-thick Co, detailed x-ray diffraction studies indicated a total interface roughness of ± 1.5 ML.[29] Consistent with this, our structural results using x-ray and TEM studies show the thickness fluctuation of ± 1 ML for 10 ML of Co. Therefore, atomic-scale structural inhomogeneities, such as defects, atomic steps, voids, and partial island formation, should play an important role for the degradation of the interface anisotropy in these ultrathin films thinner than 3 ML. Moreover, in this ultrathin-film region, thickness fluctuations as ± 1 ML cause variations in anisotropies and saturation magnetization due to the change in T_C. Therefore, it is suggested that the magnetic parameters obtained, such as anisotropy constants, represent an average of unknown variations. On the other hand, theoretical work predicted the significant broadening of the spin-wave band on the order of 10 GHz due to thickness variations such as 1–3 ML in ultrathin films.[30] The effects of structural imperfections on the spin-wave mode were examined, and thickness variations were found to cause a considerable distribution of the effective anisotropy fields. Our experimental result with a Cu overlayer shows that the spectrum width is not significantly increased with decreasing thickness down to 1.2 ML. Therefore, we conclude that thickness variations in our ultrathin films are not noticeable, from the viewpoint of the long-wavelength spin wave, although such variations should be taken into account. In addition, we note that our direct observation of a well-defined spin-wave Brillouin spectrum and its field dependence ensure the existence of ferromagnetic ordering in these ultrathin films. Therefore, our quasimonatomic Co films with $t_{\rm Co}\geqq 1.2$ ML are continuous over a range of at least several hundred nanometers. In addition, if we assume the relatively uniform structure composed of disconnected magnetic regions, such as a stripe and a plate, the long-wavelength spin wave can be detected by this Brillouin scattering, where such disconnected regions are longer than the wavelength of the spin wave of 380 nm. This localized spin wave coupled with the magnetostatic interaction might have a frequency similar to that of the uniform or surface mode in the continuous film. Unfortunately, we could not observe the wave-vector dependence of the spin-wave frequency with our experimental resolution in these ultrathin films, due to the small number of the film thickness. On the other hand, $\Delta(4\pi D_\perp M_s)_{\rm eff}$ tends to increase gradually with decreasing $t_{\rm Co}$. This quantitative result indicates that the distribution of $K_u^{(1)}$ increases gradually with decreasing $t_{\rm Co}$.

Next, we discuss the $t_{\rm Co}$ dependence of $K_u^{(1)}$ for quasimonatomic films thinner than 1.5 ML. As discussed above, the $t_{\rm Co}$ dependence of $K_u^{(1)}$ for $t_{\rm Co}\geqq 1.5$ ML with Cu overlayers can be well explained by the presence of a constant value of interface anisotropy in addition to the bulklike value of volume anisotropy. However, for $t_{\rm Co}<1.5$ ML, $K_u^{(1)}$ as well as M_s decreases rapidly with decreasing $t_{\rm Co}$. In addition to structural imperfections as discussed above, the influence of the reduction of T_C due to two-dimensionality should be taken into consideration for such decreases in both $K_u^{(1)}$ and M_s.

Unfortunately, in our experiment, the values of A obtained from the fitting of the field dependence of the spin-wave frequency have large experimental errors (several tens of percent) for quasimonatomic films thinner than 1.5 ML. Here, the effect of the exchange contribution is rather small for the field dependence of the spin-wave frequency, as shown in Fig. 5, and is equivalent to our experimental resolution of 0.5 GHz for such quasimonatomic films. Hence, it is not appropriate to discuss the role and change of the exchange interaction among Co atoms inside the film, although this exchange interaction is essentially important. However, as can be seen, $K_u^{(1)}$ for each overlayer tends to be zero at 1 ML of Co, accompanied by significant damping of the spin wave. It was previously found that ferromagnetic ordering vanished at a critical thickness of 1.6 ML in Co/Cu(100), at which thickness the in-plane anisotropy vanished simultaneously.[11] The in-plane anisotropy was pointed out to be canceled by the competition between the surface and volume anisotropy with opposite signs, and concluded to stabilize ferromagnetic ordering in the Co/Cu(100) system. On the other hand, the role of dipole interactions for the stabilization of ferromagnetic ordering was also discussed in the two-dimensional Heisenberg system.[4] Although both effects

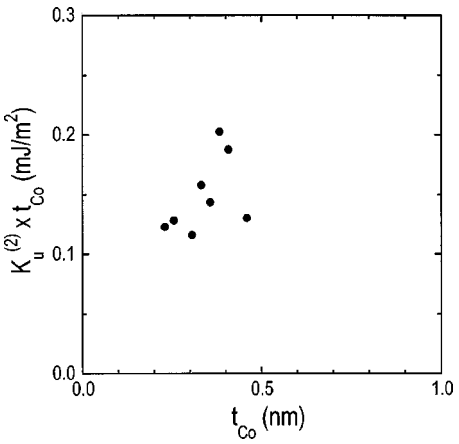

FIG. 10. Product of the second-order perpendicular anisotropy constant $K_u^{(2)}$ determined from the low-field branch of the field dependence of spin-wave frequency and t_{Co}, as a function of t_{Co}, with a Pd overlayer.

are experimentally difficult to separate, our experimental result shows directly that long-range ferromagnetic ordering with *perpendicular* anisotropy exists at RT in quasimonatomic Co/Au/Cu(111) films with thicknesses less than 1.5 ML. In this thickness range, these ultrathin films can be considered as well-defined two-dimensional systems.[12]

Finally, we discuss the behavior of the higher-order perpendicular ansiotropy $K_u^{(2)}$. From our fitting results for the field dependence of the spin-wave frequency, the contribution of $K_u^{(2)}$ appears in the low-field branch of the spin wave below H_{crit} for $t_{\mathrm{Co}} < 2.5$ ML with either Pd or Au overlayers. This result is shown in Fig. 10 for the Pd overlayer which has the largest $K_u^{(2)}$. We find that $K_u^{(2)}$ is still maintained in the quasimonatomic thickness region, whereas $K_u^{(1)}$ shows a significant degradation. Actually, the strength of $K_u^{(2)}$ becomes comparable to that of $K_u^{(1)}$ for $t_{\mathrm{Co}} \leqq 1.5$ ML. This means a significant deformation of the symmetry of the uniaxial anisotropy. Previously, we found that $K_u^{(2)}$ for 5 ML of Co increased monotonically with increasing misfit strain, while $K_u^{(1)}$ showed nonmonotonic dependence of the misfit strain.[14] In addition, we recently observed an increase in the interface contribution of $K_u^{(2)}$ with increasing misfit strain.[31] Therefore, we conclude that $K_u^{(2)}$ observed in these ultrathin films is due to the interface anisotropy induced by the epitaxial strain. This interpretation is consistent with the experimental fact that $K_u^{(2)}$ is maintained in quasimonatomic Co films thinner than 2 ML, since the first or second layer of initial Co is strongly expanded in-plane by the epitaxial growth on the Au interlayer.

IV. SUMMARY

We used a spin-wave Brillouin light scattering technique to study magnetic properties in quasimonatomic Co/Au/Cu(111) films with a 1-ML Au interlayer and with Cu, Pd, or Au overlayers. We observed well-defined spin-wave Brillouin spectra in ultrathin Co films with t_{Co} down to 1 ML. The field dependence of the spin-wave frequency directly shows long-range collective and ferromagnetic ordering in these films at room temperature. We derived uniaxial perpendicular magnetic anisotropy constants as a function of t_{Co} from the field dependence of the spin-wave frequency. From the linear relation between $K_u^{(1)} t_{\mathrm{Co}}$ and t_{Co} with $t_{\mathrm{Co}} \geqq 1.5$ ML for Cu overlayers or $t_{\mathrm{Co}} \geqq 3.0$ ML for Pd or Au overlayers, both the constant interface and volume anisotropies are determined. With the Au or Pd overlayers, we find that both anisotropies are significantly larger than those with the Cu overlayer, due to additional strain induced by the overlayer. With Au or Pd overlayers, $K_u^{(1)}$ shows a steep decrease with decreasing t_{Co} for $t_{\mathrm{Co}} \leqq 2.5$ ML, which agrees well with the significant increase in the structure-related magnetic inhomogeneity. We show that long-range ferromagnetic ordering exists with a perpendicular anisotropy in quasimonatomic Co films which is expected as a two-dimensional Heisenberg system. Finally, $K_u^{(1)}$ for all overlayers vanishes at 1 ML of Co, accompanied by significant damping of the spin wave, as well as reduction of saturation magnetization. In addition, we find that the second-order perpendicular anisotropy is still maintained in such quasimonatomic Co films.

ACKNOWLEDGMENTS

The authors are grateful to M. Imakawa and T. Hiruma of ASAHI-KOMAG Co. for their VSM measurements and S. Kondoh of ASAHI-Glass Co for his TEM observations. This research was supported in part by U.S. DOE Grant No. DE-FG02-93ER45488.

*Present address: R&D Division, ASAHI-KOMAG Co., Yonezawa, 992-1128, Japan.

[1] See various articles in *Ultrathin Magnetic Structure I & II*, edited by B. Heinrich and J. A. C. Bland (Springer-Verlag, Berlin, 1994).
[2] D. Pescia, G. Zampieri, M. Stampanoni, G. L. Bona, R. F. Willis, and F. Meier, Phys. Rev. Lett. **58**, 933 (1987).
[3] T. Beier, H. Jahrreiss, D. Pescia, Th. Woike, and W. Gudat, Phys. Rev. Lett. **61**, 1875 (1988).
[4] D. Kerkmann, J. A. Wolf, D. Pescia, Th. Woike, and P. Grünberg, Solid State Commun. **72**, 963 (1989).
[5] C. M. Schneider, P. Bressler, P. Schuster, J. Kirschner, J. J. de Miguel, and R. Miranda, Phys. Rev. Lett. **64**, 1059 (1990).
[6] N. D. Mermin and H. Wagner, Phys. Rev. Lett. **17**, 1133 (1966).
[7] D. Pescia and V. L. Pokrovsky, Phys. Rev. Lett. **65**, 2599 (1990).
[8] M. Bander and D. L. Mills, Phys. Rev. B **38**, 12 015 (1988).
[9] Z. Q. Qiu, J. Pearson, and S. D. Bader, Phys. Rev. Lett. **67**, 1646 (1991).
[10] Y. Yafet, J. Kwo, and E. M. Gyorgy, Phys. Rev. B **33**, 6519 (1986).
[11] P. Krams, F. Lauks, R. L. Stamps, B. Hillebrands, and G. Güntherodt, Phys. Rev. Lett. **69**, 3674 (1992).
[12] F. Huang, M. T. Kief, G. J. Mankey, and R. F. Willis, Phys. Rev. B **49**, 3962 (1994).
[13] A. Murayama, K. Hyomi, J. Eickmann, and C. M. Falco, J. Appl. Phys. **83**, 613 (1998).
[14] A. Murayama, K. Hyomi, J. Eickmann, and C. M. Falco, Phys. Rev. B **58**, 8596 (1998).
[15] A. Murayama, K. Hyomi, J. Eickmann, and C. M. Falco, J. Appl. Phys. **82**, 6186 (1997).

[16] C. S. Liu, S. R. Chen, W. J. Chen, and L. J. Chen, Mater. Chem. Phys. **36**, 170 (1993).
[17] F. J. A. den Broeder, W. Hoving, and P. J. H. Bloemen, J. Magn. Magn. Mater. **93**, 562 (1991).
[18] J. F. Cochran, J. Rudd, W. B. Muir, B. Heinrich, and Z. Celinski, Phys. Rev. B **42**, 508 (1990).
[19] B. Heinrich, S. T. Purcell, J. R. Dutcher, K. B. Urquhart, J. F. Cochran, and A. S. Arrott, Phys. Rev. B **38**, 12 879 (1988).
[20] M. Farle, A. Berghaus, and K. Baberschke, Phys. Rev. B **39**, 4838 (1989).
[21] M. Farle, A. Berghaus, Yi Li, and K. Baberschke, Phys. Rev. B **42**, 4873 (1990).
[22] W. B. Zeper, F. J. A. M. Greidanus, P. F. Carcia, and C. R. Fincher, J. Appl. Phys. **65**, 4971 (1989).
[23] R. L. Stamps and B. Hillebrands, Phys. Rev. B **43**, 3532 (1991).
[24] C. Chappert and P. Bruno, J. Appl. Phys. **64**, 5736 (1988).
[25] R. Jungblut, M. T. Johnson, J. aan de Stegge, A. Reinders, and F. J. A. den Broeder, J. Appl. Phys. **75**, 6424 (1994).
[26] M. Farle, Y. Henry, and K. Ounadjela, Phys. Rev. B **53**, 11 562 (1996).
[27] B. N. Engel, M. H. Wiedmann, and C. M. Falco, J. Appl. Phys. **75**, 6401 (1994).
[28] F. J. A. den Broeder, D. Kuiper, A. P. van der Mosselaer, and W. Hoving, Phys. Rev. Lett. **60**, 2769 (1988).
[29] C. H. Lee, Hui He, F. Lamelas, W. Vavra, C. Uher, and Roy Clarke, Phys. Rev. Lett. **62**, 653 (1989).
[30] R. L. Stamps, R. E. Camley, B. Hillebrands, and G. Güntherodt, Phys. Rev. B **47**, 5072 (1993).
[31] A. Murayama, K. Hyomi, J. Eickmann, and C. M. Falco (unpublished).